

# Neutral pion photoproduction off protons in the energy range $0.3 \text{ GeV} < E_\gamma < 3 \text{ GeV}$

O. Bartholomy<sup>1</sup>, V. Credé<sup>1</sup>  $\diamond$ , H. van Pee<sup>1</sup>  $*$ , A. V. Anisovich<sup>1,2</sup>, G. Anton<sup>3</sup>, R. Bantes<sup>4</sup>, Yu. Beloglazov<sup>2</sup>, R. Bogendörfer<sup>3</sup>, R. Castelijns<sup>5</sup>, A. Ehmanns<sup>1</sup>, J. Ernst<sup>1</sup>, I. Fabry<sup>1</sup>, H. Flemming<sup>6</sup>, A. Fösel<sup>3</sup>, H. Freiesleben<sup>7</sup>, M. Fuchs<sup>1</sup>, Ch. Funke<sup>1</sup>, R. Gothe<sup>4</sup>  $+$ , A. Gridnev<sup>2</sup>, E. Gutz<sup>1</sup>, S.K. Höffgen<sup>4</sup>, I. Horn<sup>1</sup>, J. Hößl<sup>3</sup>, R. Joosten<sup>1</sup>, J. Junkersfeld<sup>1</sup>, H. Kalinowsky<sup>1</sup>, F. Klein<sup>4</sup>, E. Klempt<sup>1</sup>, H. Koch<sup>6</sup>, M. Konrad<sup>4</sup>, B. Kopf<sup>6</sup>  $7$ , B. Krusche<sup>8</sup>, J. Langheinrich<sup>4</sup>  $+$ , H. Löhner<sup>5</sup>, I. Lopatin<sup>2</sup>, J. Lotz<sup>1</sup>, H. Matthäy<sup>6</sup>, D. Menze<sup>4</sup>, J. Messchendorf<sup>9</sup>  $\dagger$ , C. Morales<sup>4</sup>, D. Novinski<sup>2</sup>, M. Ostrick<sup>4</sup>, A. Radkov<sup>2</sup>, J. Reinnarth<sup>1</sup>, A. V. Sarantsev<sup>1,2</sup>, S. Schadmand<sup>9</sup>, Ch. Schmidt<sup>1</sup>, H. Schmieden<sup>4</sup>, B. Schoch<sup>4</sup>, G. Suft<sup>3</sup>, V. Sumachev<sup>2</sup>, T. Szczepanek<sup>1</sup>, U. Thoma<sup>1</sup>  $*$ , D. Walther<sup>4</sup> and Ch. Weinheimer<sup>1</sup>

(The CB-ELSA Collaboration)

<sup>1</sup> *Helmholtz-Institut für Strahlen- und Kernphysik, Universität Bonn, Germany*

<sup>2</sup> *Petersburg Nuclear Physics Institute, Gatchina, Russia*

<sup>3</sup> *Physikalisches Institut, Universität Erlangen, Germany*

<sup>4</sup> *Physikalisches Institut, Universität Bonn, Germany*

<sup>5</sup> *Kernfysisch Versneller Instituut, Groningen, Netherlands*

<sup>6</sup> *Institut für Experimentalphysik I, Ruhr-Universität Bochum, Germany*

<sup>7</sup> *Institut für Kern- und Teilchenphysik, Universität Dresden, Germany*

<sup>8</sup> *Physikalisches Institut, Universität Basel, Switzerland and*

<sup>9</sup> *Physikalisches Institut, Universität Gießen, Germany*

$\diamond$  *currently at Cornell University, USA, \* currently at* <sup>9</sup>,

$\dagger$  *currently at* <sup>5</sup>,  $+$  *currently at University of South Carolina, USA*

(Dated: 8th February 2020)

Single  $\pi^0$  photoproduction has been studied with the CB-ELSA experiment at Bonn using tagged photon energies between 0.3 and 3.0 GeV. The experimental setup covers a very large solid angle of  $\sim 98\%$  of  $4\pi$ . Differential cross sections  $d\sigma/d\Omega$  have been measured. Complicated structures in the angular distributions indicate a variety of different resonances being produced in the  $s$  channel intermediate state  $\gamma p \rightarrow N^*(\Delta^*) \rightarrow p\pi^0$ . A combined analysis including the data presented in this letter along with other data sets reveals contributions from known resonances and evidence for a new resonance  $N(2070)D_{15}$ .

PACS numbers: 14.20

The study of baryon resonances, of their masses, widths, and decay modes, is a cornerstone to improve our understanding of the internal structure of nucleons. Apart from the recently suggested exotic pentaquark state  $\Theta^+(1540)$  [1], the pattern of known baryon resonances below masses of 1.8 GeV listed by the **Particle Data Group** (PDG) [2] is generally well reproduced by present quark model calculations [3, 4, 5]. Above this mass, models predict many more resonances than have been seen experimentally. Moreover, the mass predictions of models using one-gluon exchange [3] or instanton-induced interactions [5] no longer agree. Lattice gauge calculations reproduce the masses of ground-state baryons rather well [6] and even first excited states have been simulated [7]. However the structure of baryons is still far from being understood.

Results of elastic and inelastic  $\pi N$  scattering experiments provide the largest fraction of our knowledge on the excitation spectra of the nucleon and the  $\Delta(1232)P_{33}$ . Most excited states are also reached in photonuclear reactions, yielding information on their photocouplings. The investigation of the neutral pion channel is particularly interesting since background terms from direct produc-

tion off the pion cloud or from production via  $t$ -channel exchange of pions are suppressed.

Experimental information on  $\pi^0$  photoproduction is sparse at high photon energies. Our existing knowledge is condensed into the parameterizations of SAID, a partial wave analysis program run at GWU [8, 9] and of MAID, the Mainz unitarity isobar model for pion photo- and electroproduction [10]. Most data sets cover the low-energy region or date back to the 1970s and are limited in solid angle coverage and accuracy. Here, we just quote the recent JLab data on single  $\pi^0$  photoproduction, covering the photon energy range from 434 to 1742 MeV and an angular range which varies from  $-0.89$  to  $0.15$  in  $\cos\theta_{\text{cm}}$  at the lowest, and from  $-0.79$  to  $0.89$  at the highest energy [11].

In this letter we report on a new measurement of single  $\pi^0$  photoproduction off protons covering the energy range from the  $\Delta(1232)P_{33}$  mass region up to an invariant mass of  $2.54 \text{ GeV}/c^2$ . The experiment (Fig. 1) was carried out at the tagged photon beam of the **ELectron Stretcher Accelerator** (ELSA) at the University of Bonn. Electrons were extracted at energies of 1.4 and 3.2 GeV, covering photon energies from 0.3 to 3.0 GeV, with a typ-

ical intensity of  $1\text{--}3 \times 10^6$  tagged photons/s. The photon beam hit a liquid  $\text{H}_2$  target of 5 cm length and 3 cm diameter. Charged reaction products were detected in a three-layer scintillating fiber (scifi) detector. One of the layers was straight, the fibers of the other two layers encircled the target with  $\pm 25^\circ$  with respect to the first layer. The intersection point of a proton could be reconstructed for polar angles from  $15^\circ$  to  $165^\circ$ . Charged particles and photons were detected in the Crystal Barrel detector [12]. It consisted of 1380 CsI(Tl) crystals with photodiode readout covering 98% of  $4\pi$ . A total absorption photon detector (oil Čerenkov counter, not shown in Fig. 1) placed downstream was used to determine the photon flux.

The coincidence between tagger and scifi detector provided the first-level trigger of the experiment. From the hit pattern in the Crystal Barrel detector, a fast cluster logic determined the number of 'particles' defined by clusters of contiguous crystals with individual energy deposits above 15 MeV. A second level trigger was generated for events with two or more 'particles' in the cluster logic. In the data analysis, clusters with two local maxima were split into two 'particles' sharing the total energy deposit. The offline threshold for accepted particles was set to 20 MeV. The proton kinetic energy had to exceed 35 MeV to traverse the inner two scifi layers and to produce a trigger. A proton energy of 90 MeV was needed to reach the barrel calorimeter and to deposit the minimum cluster energy of 20 MeV.

In the first step of data reduction, we required both photons to be detected in the Crystal Barrel and that not more than one candidate for the proton was found in barrel and/or inner detector. Thus, we retained events with two or three 'particles'. Proton candidates were identified by the geometrical relation of impact points in the scifi and in the barrel. In the further analysis, protons were not explicitly used but treated as missing particles. The remaining two 'particles' were treated as photons. These events were subjected to kinematic fits imposing energy and momentum conservation by fitting the  $p(\gamma, \gamma\gamma)p_{\text{missing}}$  hypothesis using one constraint (1 C) and the  $p(\gamma, \pi^0)p_{\text{missing}}$  hypothesis (2 C) for  $E_\gamma < 1.3$  GeV.

Fig. 2 shows the  $\gamma\gamma$  invariant mass spectrum after a  $10^{-4}$  confidence level cut in the 1 C kinematic fit. The  $\pi^0$  and  $\eta$  signals are observed above a small residual background. There are  $2.6 \times 10^6$  events due to  $\gamma p \rightarrow p\pi^0$ . The data is listed numerically in the Durham data base [13]. The photoproduction of  $\eta$  mesons is discussed in a subsequent letter [14].

The acceptance of the detector was determined from GEANT-based Monte Carlo simulations. It vanishes for forward protons leaving the Crystal Barrel through the forward hole, and for protons having very low lab momenta.

The absolute normalization was derived from the measured photon flux and by a comparison of our data with

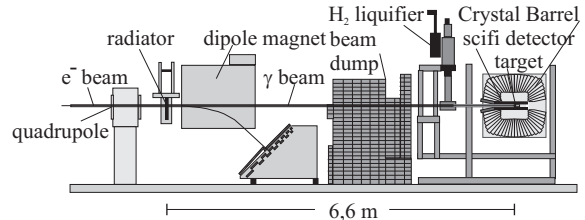


Figure 1:  
Experimental  
setup at ELSA in  
Bonn

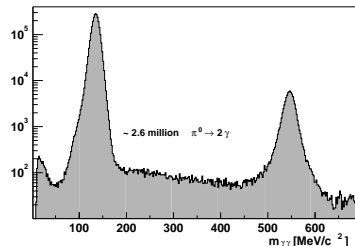


Figure 2: Spec-  
trum of invariant  
 $\gamma\gamma$  masses on a  
logarithmic scale.

SAID. For each energy channel in the tagger, the angular distributions were divided into 20 bins in  $\cos\theta_{\text{cm}}$  where  $\theta_{\text{cm}}$  denotes the emission angle of the meson in the center-of-mass system with respect to the initial photon direction. For the low energy data (below 1.3 GeV) the resulting distributions were fitted to SAID by the  $\chi^2$  method for each energy channel. The shapes of the distributions are in excellent agreement. The absolute flux normalization was determined from the SAID data base. For the high-energy data, this method could have been applied up to about 2 GeV. Above, experimental and SAID angular distributions deviate significantly. Below 2 GeV, a comparison of our angular distributions and SAID defines the absolute normalization of our photon flux, with one scaling factor over the full energy range. The uncertainty of the normalization is estimated to 5% for photon energies below 1.3 GeV and to 15% above.

The differential cross sections  $d\sigma/d\Omega$  are shown in Fig. 3. Statistical and systematic errors are added quadratically. The latter were calculated from Monte Carlo simulations of different experimental uncertainties, a shift of the photon beam by 3 mm with respect to the target center, a target shift of  $\pm 1.5$  mm in beam direction and a change in the thickness of material between barrel and inner detector corresponding to 1 mm of capton foil. The relative reconstruction efficiency error was estimated to 5%. As the angular distributions are not influenced by the flux errors, these are not included in Fig. 3. The solid line shows the result of the partial wave analysis described below. The total cross section in Fig. 4 was obtained by integration of the measured cross section and extrapolation to the non-measured region by using the results of the partial wave analysis (PWA).

The data was subjected to a coupled-channel partial wave analysis within the framework of an isobar model. Resonances are described by Breit-Wigner amplitudes, except for strongly overlapping states which are described in K-matrix formalism. Angular distributions are calculated in the spin-orbital decomposition formalism [15, 16]. The PWA method is described else-

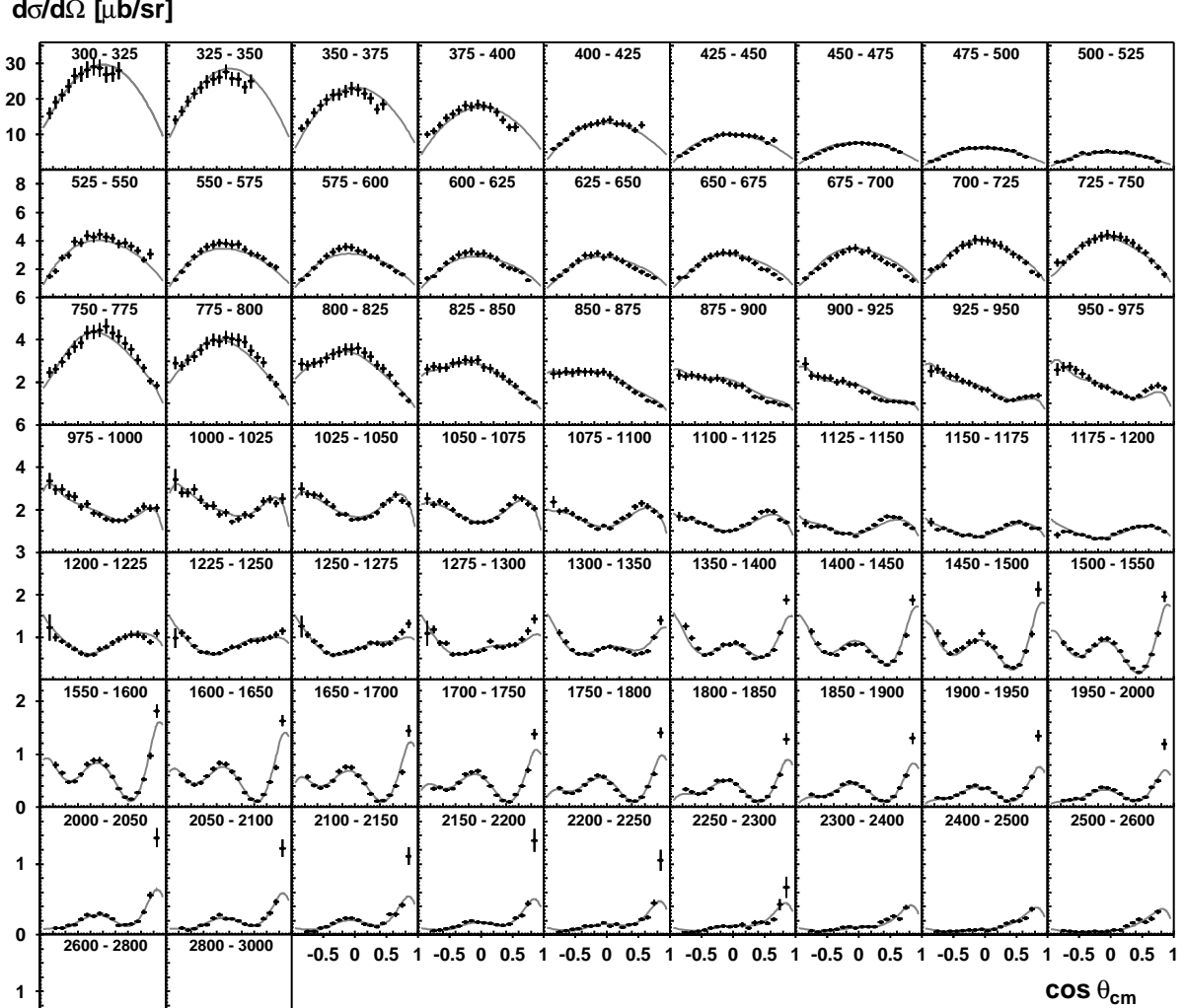


Figure 3: Differential cross sections for  $\gamma p \rightarrow p\pi^0$ . The measured data points are shown as black squares, the PWA result as a grey line. The SAID parameterization (not shown) reproduces the very forward data points. However, the agreement over the full angular range is worse.

where [17].

Along with the CB-ELSA data on photoproduction of  $\pi^0$  and  $\eta$  mesons as discussed here and in the subsequent letter [14], several other data sets served as input for the analysis: The TAPS low-energy data on  $\gamma p \rightarrow p\eta$  [18] to fix the  $\eta$  threshold; beam-asymmetry measurements of  $\pi^0$  [19, 20] and  $\eta$  [19, 21] photoproduction were used to provide additional constraints from polarization observables. The beam-asymmetry data covers the mass range from 1200 to 2000 MeV. We include data on  $\gamma p \rightarrow n\pi^+$  [22] covering the mass range from 1500 to 2150 MeV thus exploiting the different decay couplings of  $N^*$  and  $\Delta^*$  resonances to  $n\pi^+$  and  $p\pi^0$ .

The  $\chi^2$  of the final fit values for the different data sets are given in [14]. The masses, widths, helicity ratios, and contributions of different resonances to the cross section for  $\pi^0$  photoproduction from the final solution are given in Tab. I. We consider contributions to the to-

tal cross section with fractional yields (column 5) above 1–2% as established from this analysis. The sum of fractional yields is not equal to one due to interferences.

In the total cross section clear peaks are observed for the first, second, and third resonance region. A further broad enhancement can be seen at about 1900 MeV. The first resonance region is of course mainly due to the  $\Delta(1232)P_{33}$ ; the  $N(1440)P_{11}$  Roper resonance provides a small contribution of about 3–4% compared to the  $\Delta(1232)P_{33}$ . The  $A_{1/2}/A_{3/2}$  helicity ratio of excitation of the  $\Delta(1232)P_{33}$  is determined to be  $0.52 \pm 0.03$  which agrees favorably with the PDG average  $0.53 \pm 0.03$ .

The second resonance region receives approximately equal contributions from the  $N(1535)S_{11}$  and the  $N(1520)D_{13}$ . The helicity ratio  $|A_{1/2}/A_{3/2}|$  of the excitation of the  $N(1520)D_{13}$  is determined to be small ( $\leq 0.18$ ). From the couplings given by the PDG we calculate  $-(0.14 \pm 0.06)$ ; Mukhopadhyay used an effective

Table I: Masses, widths and resonance couplings, this analysis.

Resonance	M (MeV)	$\Gamma$ (MeV)	$A_{1/2}/A_{3/2}$	Fraction
N(1440)P <sub>11</sub>	1375 $\pm$ 40	380 $\pm$ 120	—	0.037
N(1520)D <sub>13</sub>	1523 $\pm$ 4	105 <sup>+6</sup> <sub>-18</sub>	0.08 $\pm$ 0.10	0.108
N(1535)S <sub>11</sub> *	1501 $\pm$ 5	215 $\pm$ 25	—	0.150
N(1650)S <sub>11</sub> *	1610 $\pm$ 10	190 $\pm$ 20	—	0.150
N(1675)D <sub>15</sub>	1690 $\pm$ 12	125 $\pm$ 20	0.06 $\pm$ 0.18	0.002
N(1680)F <sub>15</sub>	1669 $\pm$ 6	85 $\pm$ 10	-0.12 $\pm$ 0.04	0.056
N(1700)D <sub>13</sub>	1740 $\pm$ 12	84 $\pm$ 16	0.01 $\pm$ 0.20	0.001
N(1720)P <sub>13</sub>	1775 $\pm$ 18	325 $\pm$ 25	0.68 $\pm$ 0.10	0.013
N(2000)F <sub>15</sub>	1950 $\pm$ 25	230 $\pm$ 45	1.08 $\pm$ 0.60	0.002
N(2070)D <sub>15</sub>	2068 $\pm$ 22	295 $\pm$ 40	1.37 $\pm$ 0.24	0.008
N(2080)D <sub>13</sub>	1943 $\pm$ 17	82 $\pm$ 20	0.97 $\pm$ 0.28	0.000
N(2200)P <sub>13</sub>	2214 $\pm$ 28	360 $\pm$ 55	0.41 $\pm$ 0.22	0.000
$\Delta(1232)$ P <sub>33</sub> <sup>◊</sup>	1235 $\pm$ 6	135 $\pm$ 15	0.52 $\pm$ 0.03	0.820
$\Delta(1620)$ S <sub>31</sub>	1627 $\pm$ 8	118 $\pm$ 15	—	0.014
$\Delta(1700)$ D <sub>33</sub>	1686 $\pm$ 8	188 $\pm$ 18	0.94 $\pm$ 0.12	0.077
$\Delta(1905)$ F <sub>35</sub>	1970 $\pm$ 40	325 $\pm$ 50	1.32 $\pm$ 0.45	0.004
$\Delta(1920)$ P <sub>33</sub>	2032 $\pm$ 16	395 $\pm$ 50	0.35 $\pm$ 0.12	0.032
$\Delta(1940)$ D <sub>33</sub>	1910 <sup>+20</sup> <sub>-40</sub>	230 $\pm$ 45	1.20 <sup>+0.8</sup> <sub>-0.4</sub>	0.004
$\Delta(1950)$ F <sub>37</sub>	1888 $\pm$ 6	220 $\pm$ 18	0.80 $\pm$ 0.11	0.037

\* K matrix fit, pole position of the scattering amplitude in the complex plane, fraction for the total K-matrix contribution

◊ This contribution includes non-resonant background.

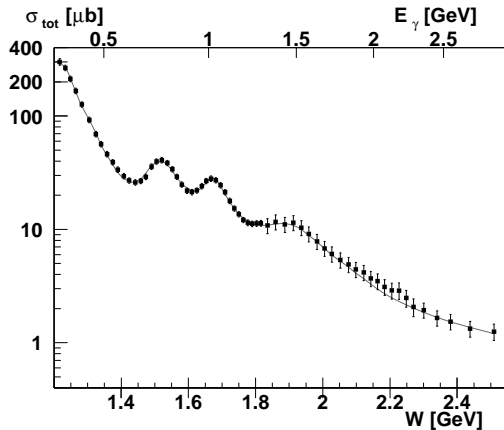


Figure 4: Total cross section for  $\gamma p \rightarrow p\pi^0$  obtained by integration of angular distributions and extrapolation into forward and backward regions using of PWA result. The solid line represents the result of the PWA.

Lagrangian approach to determine it to be  $-(0.4 \pm 0.1 \pm 0.1)$  [23]. Within  $\sim 2\sigma$  there is consistency between these values.

The third bump in the data is made up out of three major contributions. The  $\Delta(1700)$ D<sub>33</sub> provides the largest fraction ( $\sim 35\%$ ) of the peak, followed by the N(1680)F<sub>15</sub> ( $\sim 25\%$ ) and the N(1650)S<sub>11</sub> ( $\sim 20\%$ ) as extracted from K-matrix parameterization; the  $\Delta(1620)$ S<sub>31</sub> ( $\sim 7\%$ ) and the N(1720)P<sub>13</sub> ( $\sim 6\%$ ) are also observed.

In the fourth resonance region we identify the  $\Delta(1950)$ F<sub>37</sub> contributing  $\sim 41\%$  to the enhancement and the  $\Delta(1920)$ P<sub>33</sub> with  $\sim 35\%$ . The fit also requires the presence of the  $\Delta(1905)$ F<sub>35</sub> and the  $\Delta(1940)$ D<sub>33</sub>. Addi-

tionally, evidence is found for a new resonanc N(2070)D<sub>15</sub> ( $\sim 9\%$ ) and indications for a new state N(2200)P<sub>13</sub> which will be discussed in the subsequent letter. The high-energy region is dominated by  $\rho$ - $\omega$  exchange in the  $t$  channel as can be seen by the forward peaking in the differential cross sections.

We have reported new data on the photoproduction of neutral pions off protons over the full baryon resonance region. The data extends the existing data base in larger solid angle coverage and in energy. A partial wave analysis of the data presented here and elsewhere [14, 17] decomposes the data into contributions from a large number of N\* and  $\Delta^*$  resonances.

We thank the technical staff at ELSA and at all the participating institutions for their invaluable contributions to the success of the experiment. We acknowledge financial support from the Deutsche Forschungsgemeinschaft (DFG). The collaboration with St. Petersburg received funds from DFG and the Russian Foundation for Basic Research. B. Krusche acknowledges support from Schweizerischer Nationalfond. U. Thoma thanks for an Emmy Noether grant from the DFG. A. V. Anisovich and A. V. Sarantsev acknowledge support from the Alexander von Humboldt Foundation. This work comprises part of the PhD theses of O. Bartholomy and H. van Pee.

- [1] For a review see E. Klempt, arXiv:hep-ph/0404270.
- [2] K. Hagiwara *et al.*, Phys. Rev. D **66** (2002) 010001.
- [3] S. Capstick and N. Isgur, Phys. Rev. D **34** (1986) 2809.
- [4] L. Y. Glozman *et al.*, Phys. Rev. D **58** (1998) 094030.
- [5] U. Löring, B. C. Metsch and H. R. Petry, Eur. Phys. J. A **10** (2001) 395, 447.
- [6] R. D. Young *et al.*, Nucl. Phys. **109A** (2002) 55.
- [7] D. G. Richards *et al.*, arXiv:nucl-th/0206049.
- [8] R. A. Arndt *et al.*, <http://gwadac.phys.gwu.edu>.
- [9] R. A. Arndt *et al.*, Phys. Rev. C **66** (2002) 055213.
- [10] W. T. Chiang *et al.*, Phys. Rev. C **68** (2003) 045202.
- [11] P. Heimberg *et al.*, INPC 2001, Berkeley, California
- [12] E. Aker *et al.*, Nucl. Instrum. Meth. A **321** (1992) 69.
- [13] <http://durpdg.dur.ac.uk/hepdata/reac.html>.
- [14] V. Crede *et al.*, subsequent letter.
- [15] W. Rarita and J. S. Schwinger, Phys. Rev. **60** (1941) 61.
- [16] V. V. Anisovich *et al.*, Phys. Atom. Nucl. **57** (1994) 1595.
- [17] A. V. Anisovich, E. Klempt, A. V. Sarantsev and U. Thoma, in preparation.
- [18] B. Krusche *et al.*, Phys. Rev. Lett. **74** (1995) 3736.
- [19] We thank the GRAAL collaboration for providing their data to us prior to publication.
- [20] A. A. Belyaev *et al.*, Nucl. Phys. B **213** (1983) 201. R. Beck *et al.*, Phys. Rev. Lett. **78** (1997) 606. D. Rebreyend *et al.*, Nucl. Phys. A **663** (2000) 436.
- [21] J. Ajaka *et al.*, Phys. Rev. Lett. **81** (1998) 1797.
- [22] K. H. Althoff *et al.*, Z. Phys. C **18** (1983) 199. E. J. Durwen, BONN-IR-80-7 (1980). K. Buechler *et al.*, Nucl. Phys. A **570** (1994) 580.
- [23] N. P. Mukhopadhyay, N. Mathur, Phys. Lett. B **444** (1998) 7.